Int. J. Electrochem. Sci., 11 **(2016)** 4110 - 4119

International Journal of
ELECTROCHEMICAL
SCIENCE
www.electrochemsci.org

In-situ Scanning Micro-Electrochemical Characterization of Corrosion Inhibitors on Copper

Bowei Zhang[1,2], *Junsheng Wu*[1,*], *Dongdong Peng*[1], *Xiaogang Li*[1], *Yizhong Huang*[2]

[1] Institute of Advanced Materials and Technology, University of Science and Technology Beijing, Beijing, China
[2] School of Materials Science and Engineering, Nanyang Technological University, Singapore
[*]E-mail: wujs@ustb.edu.cn

Received: 14 January 2016 / *Accepted:* 8 March 2016 / *Published:* 1 April 2016

In-situ scanning vibrating electrode technique (SVET) combined with other techniques (such as electrochemical impedance spectroscopy (EIS), atomic force microscopy (AFM) and X-ray photoelectron spectroscopy (XPS)) was used to investigate the efficiency of the mixed compound of 3-amino-1, 2, 4-triazole (ATA) and sodium molybdate (SM) as a corrosion inhibitor for copper in 3.5% NaCl solution in comparison with benzotriazole (BTA). The results indicate that copper shows extremely higher corrosion resistance in 3.5% NaCl solution with the presence of ATA-SM inhibitor than BTA. This is due to the reaction of ATA with copper allowing the formation of a thin film incorporated with MoO_4^{2-} ion precipitates on the surface of copper, which provides strong cathodic efficiency and thus is considerably protective.

Keywords: In-situ, SVET, ATA-SM, inhibitor, copper

1. INTRODUCTION

Copper, one of the most widely applied materials around the world, is suffering from the corrosion of various environments. Therefore, corrosion prevention on copper is a key point if we want to expand its applications. Generally, the corrosion can hardly prevented completely due to the complex working environments so that we need to minimize the corrosion rate. Inhibitors can play the role of making the corrosion slower with only a small amount.

During the past decades, variety of methods have been developed and engaged in the study of corrosion and prevention performance. Recently, local electrochemical techniques are becoming more popular and effective investigating the mechanisms of corrosion behavior in aqueous environments, as well as in in-situ characterizing surface reactivity[1, 2]. For example, BTA, a commonly used

doi: 10.20964/110367

inhibitor, is able to reduce the corrosion of copper in aqueous solutions with chloride ions. However, the interactions between inhibitors interact and materials are still unclear [3-8]. Scanning vibrating electrode technique (SVET) is a powerful electrochemical instrument that allows the direct observation of the evolution of sample surfaces when in contact with environment [9-14].

It is known that BTA provides the better inhibiting efficiency of corrosion for copper in aqueous chloride environments than the individual ATA and sodium molybdate inhibitors [15-18]. However, its protective mechanism of Cu (I)- BTA film formed on the surface of copper has not been completely understood so far. In addition, the toxicity of BTA restricts its application currently. Therefore, searching high-efficiency and nontoxic inhibitors to replace BTA has been a tendency in this field. 3-amino-1, 2, 4-triazole (ATA) is considered as a replacement of BTA as an effective inhibitor on copper [19-25]. Given the existence of synergistic effect between BTA and molybdate, there should be similar effect between ATA and molybdate due to the analogous structure of ATA AND BTA [26, 27]. The aim of the present work is to investigate the inhibiting properties of the mixture of ATA and sodium molybdate (ATA- SM) and evaluate the performance by comparing with that of BTA.

2. EXPERIMENTAL

2.1. Materials

In the present work, pure copper sheets (99.99% purity, 10mm× 10mm× 3mm) were used for the electrochemical, AFM and XPS experiments. The specimens were polished with emery paper up to 2000 grade, and then degreased in ethanol followed by rinsing using deionized water and finally dried in vacuum oven. Additional polishing of the samples for AFM test was carried out in electrolytic polishing solution. The investigated inhibitors were all supplied by Sigma-Aldrich, Singapore. The aggressive electrolyte was 3.5wt% NaCl solution.

2.2. Methods

2.2.1. Scanning Vibrating Electrode Technology (SVET)

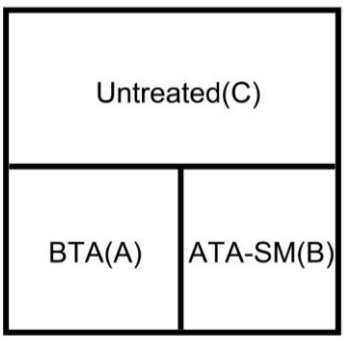

Figure 1. Distribution of different film-forming areas

Fig. 1 shows the schematic diagram of the specimen which is divided into 3 sections —BTA film section (A), ATA-SM film section (B) and untreated section (C). Section B and C were sealed by sealing film when the specimen was immersed into 10 mmol/L BTA solution for 24 hours so that the section A was covered by BTA film. The same procedure was conducted to form ATA-SM film on the section B. After the completion of film formation, SVET experiments were subsequently conducted in 3.5wt% NaCl solution respectively at 0 hour, 24hours, 48hours and 72 hours later and the specimen was immersed in 3.5% NaCl solution during the testing intervals. An Ec-lab workstation was used for SVET analysis. SVET test was conducted in the similar three-electrode system to EIS test where the counter electrode was built-in the workstation. Testing area is 300mm× 300mm and moving step of the probe is 100μm.

2.2.2. Electrochemical Impedance Spectroscopy (EIS)

Electrochemical impedance spectroscopy is widely used to characterize the anti-corrosive properties and clarify the protective mechanism of inhibitors [15]. This technology allows not only the comparison between different systems but also can provide important information on kinetics of evolution of the film degradation and corrosive activities during immersion in corrosive media [16].

EIS test was conducted in three-electrode system after one hour immersion in the solutions using an Ec- lab workstation produced by Princeton Instruments. A Pt foil was used as the counter electrode and a saturated calomel electrode (SCE) with a Luggin capillary as the reference. All potentials are reported versus SCE. Working electrode was mounted by epoxyresinwith the exposed area of 1 cm^2 (10 mm× 10 mm). EIS experiments were performed at the open circuit potential over a frequency range from100 kHz to 10 mHz and amplitude of the sinusoidal signal was set to be ±10 mV.

2.2.3. Atomic Force Microscopy (AFM)

Two specimens were placed into 3.5% NaCl solutions with and without 10 mmol L^{-1} inhibitors for 72 hours, respectively before the characterization in AFM. The morphology of the specimens was observed by a contacted AFM (Vecco Nanoscope5) with a silicon nitride (Si_3N_4) probe. Testing area is 80μm× 80μm.

2.2.4. X-ray photoelectron spectroscopy (XPS)

The specimen was immersed into the ATA-SM solution for 24 hours before XPS analysis was carried out using an Al Kα X-ray source at 10kv, 150W with a pressure below 1.33×10^{-6} Pa. XPS data was interpreted using XPS peaks software. Charge referencing was determined by setting the main C 1s component at 285.0 eV. The surface composition (in atomic%) of the specimen was identified by considering the integrated peak areas of N 1s, Mo $3d_{5/2}$, Cu $2p_{3/2}$ and their respective sensitivity factors provided by the analyzing software.

3. RESULTS AND DISCUSSION

3.1. Scanning Vibrating Electrode Technology (SVET)

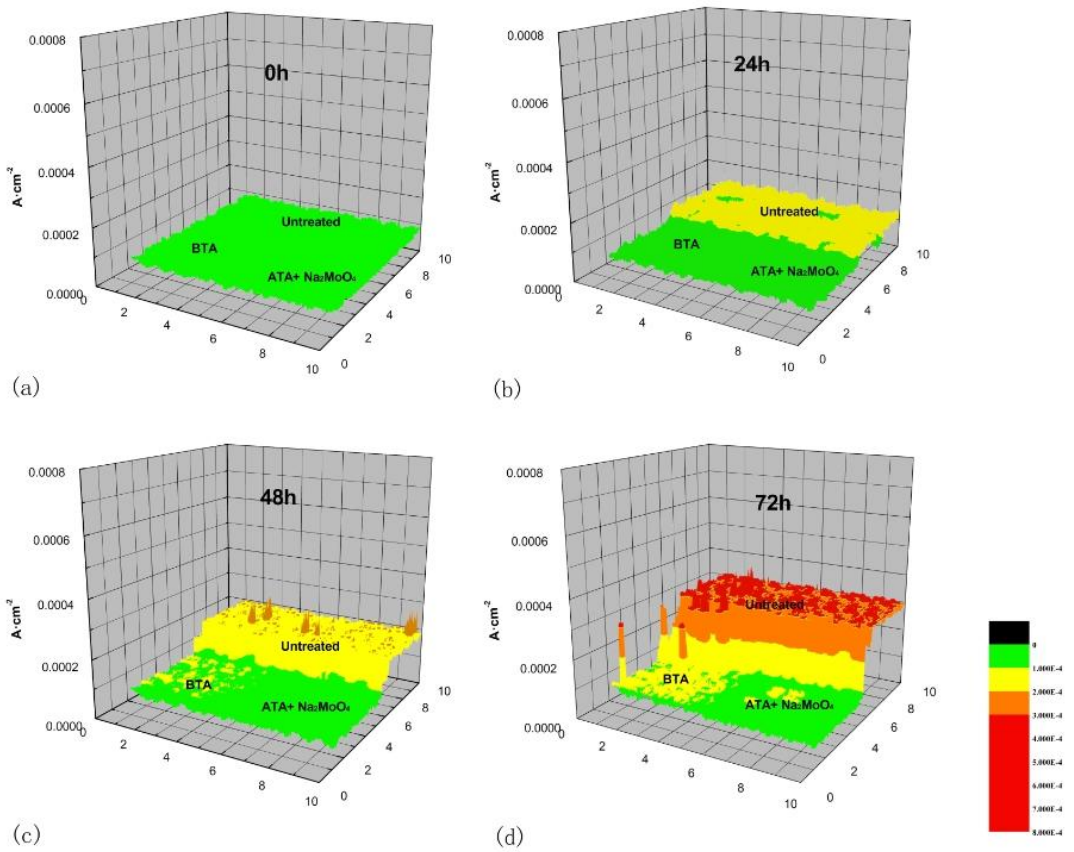

Figure 2. Distribution of current density on the copper surface immersed in 3.5% NaCl solution coated with and without different inhibitors after 0h, 24hours, 48hours and 72hours

Fig. 2 shows the evolution of current density distribution on the sample surface over 72 hours' immersion in the solution obtained in situ by using Scanning Vibrating Electrode Technology (SVET). Slight and homogeneous increase of the surface current density is seen across the untreated area (i.e. surface C) after 24 hours, indicating the onset of corrosion (Fig. 2a). The surface current density rises up much higher with further immersion of 24 hours suggesting more serious occurrence of corrosion (Fig. 2b), which becomes considerably worse after another 24 hours (Fig. 2c). In contrast, very low current density was detected at very few regions on the surface 'A' until it was immersed in the solution with BTA inhibitor for 48 hours. However, the surface 'B' sustains even more intact than the surface 'A' immersed in the solution with ATA- SM, where almost no corrosion occurs throughout 72 hours. Only a little amount of current was detected in a couple of regions, much smaller than the current generated from the surface 'A'. Therefore, we can conclude that ATA- SM is more protective to the copper surface than BTA, as proven by EIS measurement below.

3.2. Electrochemical Impedance Spectroscopy (EIS)

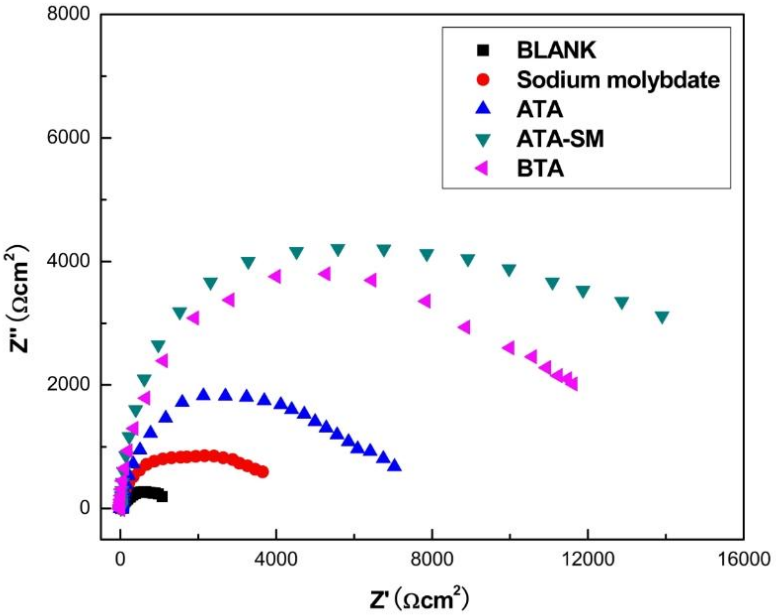

Figure 3. Nyquist plots for the Cu electrode after one hour immersion in a 3.5% NaCl solution without inhibitor and with different 10 mmol L^{-1} inhibitor for each group

Nyquist diagrams of copper in 3.5% NaCl solution with and without 10 mmol L^{-1} inhibitors are shown in Fig.3. The specimens with inhibitors present higher impedance values compared to the blank specimen. In addition, all the impedance spectra above do not show any new capacitive or inductive loops at low frequency, which implies that all the inhibitors are mixed-type at copper-solution interface. Their inhibition behavior is considered as physical or chemical coverage on the surface of copper electrode [28]. It is well known that the diameter of the capacitive loop in Nyquist diagram represents the charge transfer resistance (Rt) of the working electrode [16]. Larger the diameter suggests higher charge transfer resistance (Rt), which means the charge transfer reaction (copper dissolution reaction) has a relative lower speed. Of all the inhibitors tested, ATA-SM adsorbed on copper has largest diameter and therefore it provides the best corrosion resistance to copper.

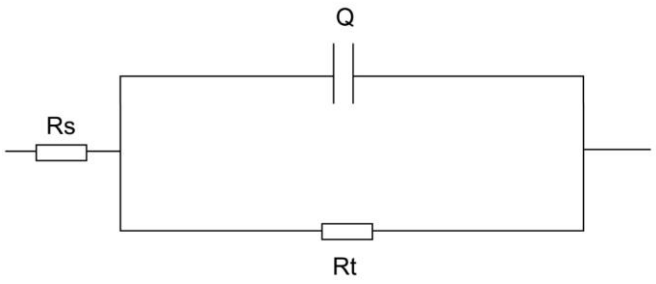

Figure 4. Equivalent circuit of copper in 3.5 NaCl solutions with and without different inhibitors

Table 1. Electrochemical impedance parameters of copper 3.5 NaCl solutions with and without different inhibitors

	Rt/（kΩ·cm^{-2}）	Q/（F·cm^{-2}）	N
Blank	7.4	8.472E-4	0.63
Sodium molybdate	40.26	9.16E-5	0.68
ATA	106.2	2.54E-5	0.73
BTA	168.5	4.83E-6	0.91
ATA-SM	183.2	2.35E-6	0.95

A simulated equivalent circuit is used to interpret the EIS experimental data through. In this stimulation, the theoretical film and double layer capacitances were replaced with the constant phase element (Q) which can denote every standard electrical element through the variation of the Q factor n between -1 and 1 [18]. Q performs a pure resistance behavior when n is 0 and a capacitance behavior when n> 0.6. The equivalent circuit used for simulating the experimental data is shown in Fig. 4. The impedance parameters calculated with ZSimpWin are given in Table 1.

The capacitance values decrease for each inhibitor group compared to the blank one. The decrease in Q resulting from an increase in the thickness of double-layer or a decrease in local dielectric constant indicates that inhibitors perform by adhering tightly to the copper surface. The Rt value in ATA- SM system turns out to be excellent since it is comparable to the reported high-efficiency inhibitors at the same magnitude. Consequently, the lowest capacitance value of ATA-SM as well as its highest Rt value demonstrates that it offer the most excellent corrosion protection to the copper specimen.

The deviation parameter n depends on the surface morphology of the electrode. The n values in the range of 0.6-0.76 for Blank, Na_2MoO_4, ATA groups are due to the rough surface of the electrodes. The corresponding n values for ATA-SM is 0.95, which is slightly higher than that of BTA with 0.91 and some reported results [28-30], suggesting the films have formed on the copper surface so that high inhibition efficiencies are achieved. Take the values of Rt and Q into consideration, the conclusion that ATA-SM performs the most effectively and protectively on copper is convincing.

3.3. Atomic Force Microscopy (AFM)

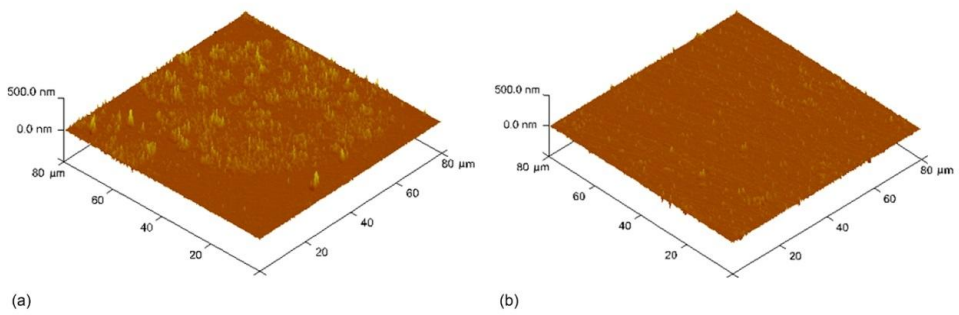

Figure 5. AFM images of the copper surface: (a) after 24 hours' immersion in 3.5% NaCl solution without inhibitor; (b) after 24 hours' immersion in 3.5% NaCl solution with ATA-SM

The effective protection of inhibitors to the copper surface was also demonstrated by AFM observation. As an example, Fig. 5 shows two AFM images of two identical samples after 24 hours' immersion in 3.5% NaCl solution without (Fig. 5a) and with (Fig. 5b) inhibitors. The image of untreated sample in Fig. 5a appears a very rough surface consisting of plenty of etching pits with the roughness measured to be approximately 336nm (Fig. 5a). In contrast, Fig. 5b shows a fairly smooth surface with the roughness of around 92nm. This result indicates that protective film composed of inhibitors has covered the surface of the sample to inhibit the corrosive reactions. In addition, those etching pits observed in Fig. 5a are possibly due to the pitting corrosion caused by the precipitation of impurities or the defects on the surface.

3.4. X-ray photoelectron spectroscopy (XPS)

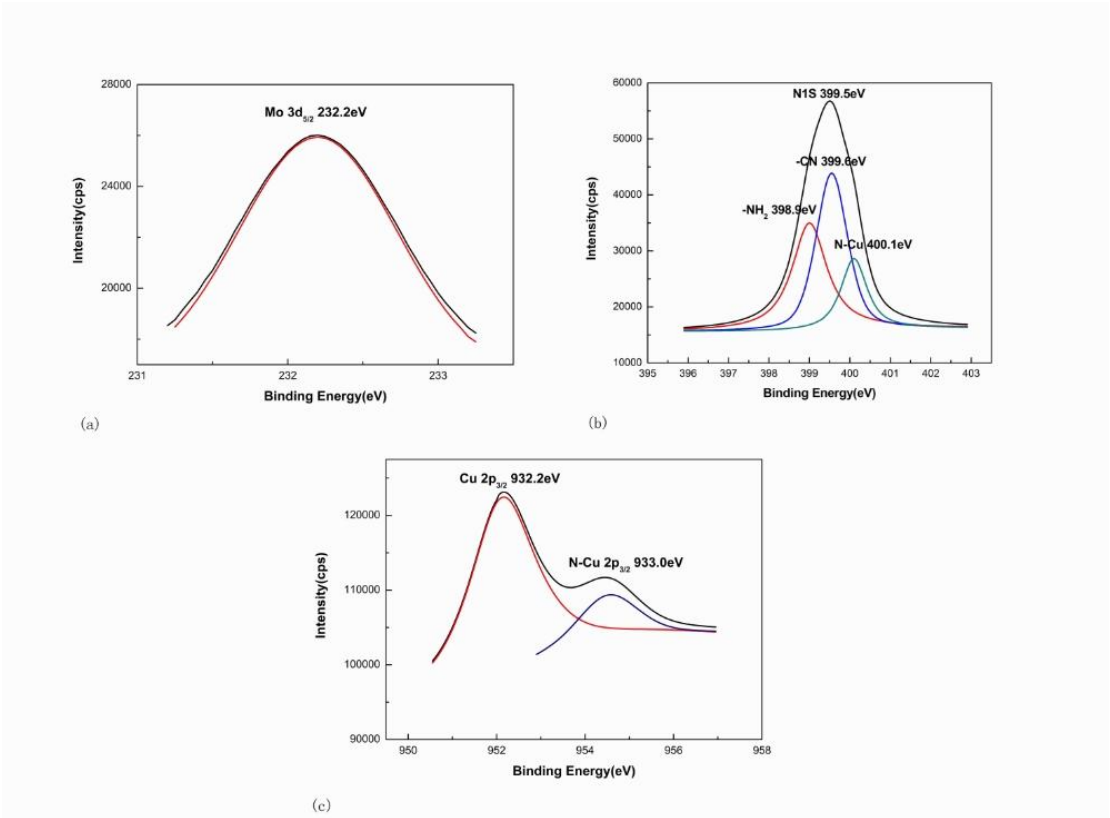

Figure 6. XPS spectrum of main elements in inhibition film on the copper surface after 48 hours

Table 2. Binding energies (eV) of main elements in inhibition film on the copper surface

	1	2	3
N 1s（eV）	**398.9**	**399.5**	**400.1**
Cu $2p_{3/2}$（eV）	**932.2**	**933.0**	
Mo $3d_{5/2}$（eV）	**232.2**		

Table 3. Area of peak of main elements and their relative sensitivity factors

	N	Cu	Mo
I_i	**5963**	**67331**	**6043**
S_i	**0.477**	**5.321**	**3.321**
I_i/S_i	**12505**	**12654**	**1819**

Except for the evaluation of the performance for each inhibitor, X-ray spectroscopy was employed to investigate the protection mechanism of ATA- SM system. Fig. 6 shows the N 1s, Mo $3d_{5/2}$ and Cu $2p_{3/2}$ XPS peaks measured on the surface of copper sample after a 48-hour film-forming period. The values of bonding energy are summarized in Table 2. The peak areas of main elements in the film and their relative sensitivity factors are presented in Table 3.

A Mo $3d_{5/2}$ peak and three N 1s peaks are identified in XPS spectra, which indicate that ATA-SM film has formed on the surface of copper. The binding energy of Mo $3d_{5/2}$ peak is measured to be 232.2 eV, which is attributed to the element of Mo in Na_2MoO_4 mixed compound [19]. The only peak of Mo indicates that there should be no chemical interaction between Na_2MoO_4 and Cu, suggesting the physical absorption of Na_2MoO_4. In contrast, there are three peaks of N: The N 1s peaks at 398.9 eV and 399.5 eV correspond to the amino and cyan in the molecule of ATA, respectively and the peak at 400.1 eV to the N atom bonded with Cu atoms [31]. The Cu $2p_{3/2}$ peak at 932.2 eV corresponds to metallic Cu atoms while the Cu $2p_{3/2}$ peak at 933.6 eV is associated with the oxide state. However, the Cu $2p_{3/2}$ peak energy is identified to be 933.0 eV, which is due to the attribution from the Cu atoms which are bonded to the ATA molecules [32]. The relative element ratio can be derived from the following equation:

$$n_i:n_j = (I_i/S_i): (I_j/S_j) \quad (1)$$

where n_i/n_j is the ratio of elements i and j. I_i and I_j represent the XPS signal intensity for element i and j while S_i and S_j represent the sensitivity factor of element i and j,respectively.

The ratio of N, Cu and Mo atoms (n_N: n_{Cu}: n_{Mo}) is 0.99: 1: 0.144 calculated from Table 3, which is an approximate value of 7: 7: 1. This result demonstrates that the main composition of the film is ATA while MoO_4^{2-} is much less than ATA. Therefore, ATA molecules adsorb onto the copper surface where they react with copper forming a thin layer of film incorporated with MoO_4^{2-} ion precipitates. It is these MoO_4^{2-} ions that are responsible for the corrosion reduction of copper due to their strong oxidation/cathodic efficiency.

4. CONCLUSIONS

The corrosion protection efficiency and the stability of the films formed by the reaction of ATA-SM and BTA with copper in 3.5% NaCl solutions for 72 hours were studied using scanning vibrating electrode technology (SVET) in combination with other techniques. The mixed compound of ATA and sodium molybdate is proved to be an excellent corrosion inhibitor for copper in chloride

solutions, with a better protection than BTA. ATA-SM suppresses the anodic reaction of copper owing to the protective film formed on the surface of copper. The results demonstrate that ATA molecules adsorb onto the copper surface to form a protective film layer enriched with MoO_4^{2-} ions, which is responsible for the corrosion reduction of copper.

ACKNOWLEDGEMENT
This work was supported by National Natural Science Foundation of China (grant no. 50701006 and51271031),Fundamental Research Funds for the Central Universities (FRF-SD-12-027A), Star-up funding in NTU (Grant No.M4010992), Tier 1 (AcRF grant MOE Singapore Grant No. 4080293).

References

1. R. Oltra，V. Maurice，R. Akid，P. Marcus, Local Probe Techniques for Corrosion Research, Elsevier, Philadelphia, PA (2014).
2. P. Marcus，Corrosion Mechanisms in Theory and Practice, Third Edition，CRC Press，Boca Raton (2011).
3. Z. Chen, L. Huang, G. Zhang, Y Qiu, X Guo, *Corrosion Science*, 65 (2012) 214.
4. D.Patel, M.Jain, S.R.Shah, R.Bahekar, P.Jadav, B.Darji, Y.Siriki,D.Bandyopadhyay, A.Joharapurkar, S.Kshirsagar, *ChemMedChem*, 6 (2011) 1011.
5. J. Izquierdo, L. Nagy, J.J. Santana, G. Nagy, R.M. Souto, *Electrochimica Acta*,58 (2011) 707.
6. M.Finšgar, I.Milošev, *Materials and Corrosion*, 62 (2011) 956.
7. A. Kokalj, N. Kovačević, S. Peljhan,M. Finšgar, A.Lesar, I.Milošev, ChemPhysChem, 12 (2011) 3547.
8. H. Gerengi, P. Slepski, G. Bereket, *Materials and Corrosion*, 64 (2013) 1024.
9. H.E. Jamil, A. Shriri, R. Boulif, C. Bastos, M.F. Montemor, M.G.S.Ferreira, *Electrochimica Acta*, 49 (2004) 2753.
10. G. Williams, H. ap. Llwyd Dafydd, R. Grace, *Electrochimica Acta*, 109 (2013) 489.
11. B.P. Wilson, J.R. Searle, K. Yliniemi, D.A. Worsley, H.N. McMurray, *Electrochimica Acta*, 66 (2012) 52.
12. G. Williams, K. Gusieva, N. Birbilis, *Corrosion*, 68 (2012) 489.
13. A. Alvarez-Pampliega, M.G. Taryba, K. Van den Bergh, J. De Strycker, S.V. Lamaka, H. Terryn, *Electrochimica Acta*, 102 (2013) 319.
14. G. Williams, H.N. McMurray, R. Grace, *Electrochimica Acta*, 55 (2010) 7824.
15. M Finšgar, I Milošev, *Corrosion science*, 52 (2010) 2737.
16. T. Kosec, D.K. Merl, I. Milošev, *Corrosion Science*, 50 (2008) 1987.
17. P. Yu, D.M. Liao, Y.B. Luo, Z.G. Chen, *Corrosion*, 59 (2003) 314.
18. N. Bellakhal, M. Dachraoui, *Materials chemistry and physics*, 85 (2004) 366.
19. B.D. Mert, M.E. Mert, G. Kardaş, B. Yazıcı, *Corrosion Science*, 53 (2011) 4265.
20. E.S.M. Sherif, *Int. J. Electrochem. Sci*., 6 (2011) 1479.
21. M. Quraishi, Corrosion Science, 70 (2013) 161.
22. M. Tourabi, K. Nohair, M. Traisnel, C. Jama, F. Bentiss, *Corrosion Science*, 75 (2013) 123.
23. A.Zarrouk, B. Hammouti, S.S. Al-Deyab, R. Salghi, H. Zarrok, C. Jama, F. Bentiss, *Int. J. Electrochem. Sci.*, 7 (2012) 5997
24. F. Eghbali, M.H. Moayed, A. Davoodi, N. Ebrahimi, *Corrosion Science*, 53 (2011) 513.
25. X. Li, S. Deng, H. Fu, *Corrosion Science*, 53 (2011) 2748.
26. M.M. Antonijevic, M.B. Petrovic, *Int. J. Electrochem. Sci*., 3 (2008) 1.
27. D.Q. Zhang, H.Goun Joo, K.Yong Lee, *Surface and Interface Analysis*, 41 (2009) 164.
28. H. Ma, S. Chen, B. Yin, S. Zhao, X. Liu, *Corrosion Science*, 45 (2003) 867.

29. H.O. Curkovic, E. Stupnisek-Lisac, H. Takenouti, *Corrosion Science*, 51 (2009) 2342.
30. M.A. Amin, *Journal of applied electrochemistry*, 36 (2006) 215.
31. M. Finšgar, *Corrosion*, 77 (2013) 350.
32. M. Finšgar, D.K. Merl, *Corrosion Science*, 83 (2014) 164.